

# Bias-controlled sensitivity of ferromagnet/semiconductor electrical spin detectors

S. A. Crooker<sup>1\*</sup>, E. Garlid<sup>2</sup>, A. N. Chantis<sup>1</sup>, D. L. Smith<sup>1</sup>, K. S. M. Reddy<sup>3</sup>, Q. Hu<sup>2</sup>, T. Kondo<sup>2</sup>, C. J. Palmstrøm<sup>3,4</sup>, P. A. Crowell<sup>2</sup>

<sup>1</sup>Los Alamos National Laboratory, Los Alamos, NM 87545

<sup>2</sup>School of Physics and Astronomy, University of Minnesota, Minneapolis, MN 55455

<sup>3</sup>Dept. of Chemical Engineering & Materials Science, University of Minnesota and

<sup>4</sup>Depts. of Electrical & Computer Engineering and Materials, University of California, Santa Barbara, CA 93106

(Dated: June 30, 2022)

Using Fe/GaAs Schottky tunnel barriers as electrical spin detectors, we show that both the magnitude and sign of their spin-detection sensitivities are widely tunable with voltage bias applied across the Fe/GaAs interface. Electrons with fixed polarization in GaAs can be made to induce either positive or negative voltage changes at spin-detection electrodes, and some detector sensitivities can be enhanced over ten-fold with applied bias. Experiments and theory establish that this tunability derives from the interplay between two physical processes: 1) the bias dependence of the tunneling spin polarization (a property of the Fe/GaAs interface), and 2) the bias dependence of spin transport in the semiconductor, which can dramatically enhance or suppress spin-detection sensitivities.

An all-electrical scheme for efficient detection of spins is an essential component of most “semiconductor spintronic” device proposals [1, 2], and recent demonstrations of electrical spin injection and detection in GaAs [3, 4, 5], silicon [6, 7], and graphene [8] have motivated a desire to understand how bulk and interfacial spin transport contribute to device performance. However, while the need for optimizing spin injection is widely recognized, the interplay of mechanisms that govern electrical spin *detection* have only begun to be explored [2, 4, 9].

Drawing from studies of all-metal spin-transport devices [10, 11], recent work on lateral devices with semiconductor channels has relied on spin-polarized electron tunneling through barriers formed at ferromagnet-semiconductor interfaces, to avoid the “conductivity mismatch problem” of ohmic contacts [12, 13]. However, tunneling typically introduces a strong dependence of polarization on applied voltage bias. In lateral Fe/GaAs structures, the spin polarization injected into GaAs channels varied markedly with the bias applied across the source electrode and unexpectedly inverted sign at finite bias [5]. In a related study, tunneling magnetoresistances through vertical Fe/GaAs/Fe trilayers also inverted sign when one interface was epitaxial [14].

As a result, polarized tunneling through ferromagnet-semiconductor interfaces has received much theoretical attention. For example, Dery and Sham considered polarization inversion by tunneling from bound states near thin Schottky barriers [15], while Chantis *et al.* described an inversion due to minority spin resonances at Fe/GaAs(001) interfaces [16]. In addressing these theories, there is a critical need to separate interfacial spin tunneling effects from the effects of spin transport due to electric fields [17, 18] in the semiconductor bulk.

We demonstrate here that the bias dependence of spin-polarized tunneling in combination with electric-field driven spin transport can be used to control the sensitiv-

ity of spin-*detection* in lateral Fe/GaAs structures, which we define as the voltage change  $\Delta V_d$  induced at a spin-detection electrode by an additional, remotely-injected spin polarization. By tuning the voltage bias  $V_d$  applied across a Fe/GaAs detector, we control both the *magnitude* and *sign* of its spin-detection sensitivity,  $\Delta V_d$ . Both experiments and theory reveal that  $\Delta V_d$  can differ significantly from the polarization of the tunneling current, due to spin drift and diffusion effects in the semiconductor channel. Finally, we show that in multi-terminal devices a spin-detector’s sensitivity can be controlled – and optimized – independently from the details of spin injection at a source electrode, providing much freedom and flexibility in device design.

Fig. 1(a) shows a typical device. Epitaxially-grown Fe/GaAs structures are processed into lateral spin-transport devices having five  $10 \times 50 \mu\text{m}$  Fe contacts (#1-5) on a  $2.5 \mu\text{m}$  thick *n*-type GaAs channel [5]. A Schottky tunnel barrier is formed at the interface between Fe and a highly-doped  $n^+$  interfacial layer of GaAs [19]. Devices from two wafers are discussed (denoted A and B, with  $n=3.5$  and  $2.0 \times 10^{16} \text{ cm}^{-3}$ ). They are characteristic of structures for which the polarization inverts under forward- and reverse source bias, respectively.

To measure the spin-detection sensitivity of these Fe/GaAs electrodes, a constant current  $j$  establishes a voltage bias  $V_d$  across a Fe/GaAs detector interface (contact #4 in Fig. 1). From [13],  $V_d = \frac{j}{4} \left[ \left( \frac{1}{G_{\uparrow}} + \frac{1}{G_{\downarrow}} \right) + \left( \frac{1}{G_{\uparrow}} - \frac{1}{G_{\downarrow}} \right) P_j \right]$ , where  $P_j = (j_{\uparrow} - j_{\downarrow})/j$  is the tunneling current polarization, and  $j_{\uparrow, \downarrow}$  and  $G_{\uparrow, \downarrow}$  are the majority- and minority-spin tunneling currents and conductances. A weak, circularly-polarized, 1.58 eV pump laser is focused to a stripe  $10\text{-}20 \mu\text{m}$  away from contact 4, optically injecting a small, constant spin polarization into the channel. This polarization, oriented initially along  $\pm \hat{z}$ , drifts and diffuses laterally and is tipped into the minority or majority spin direction

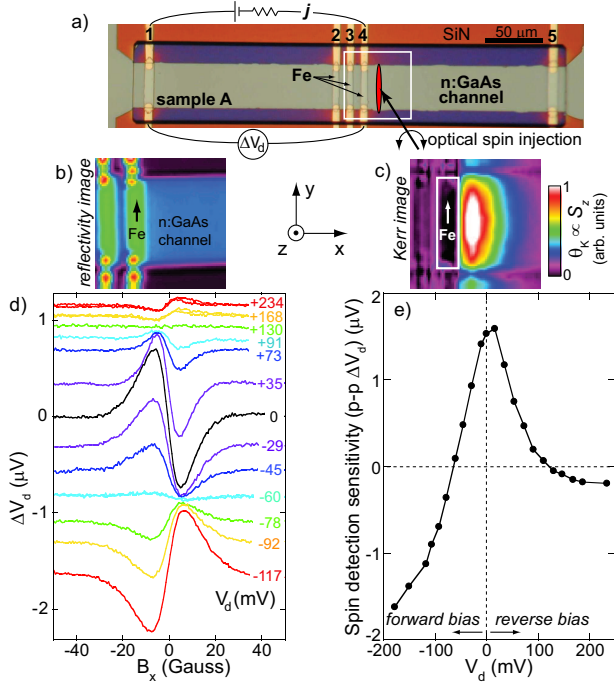


FIG. 1: a) Lateral spin transport device A and the spin detection experiment. Current  $j$  establishes a voltage  $V_d$  across a Fe/GaAs detector interface (contact 4). Changes ( $\Delta V_d$ ) due to a remote, optically-injected spin polarization reveal the detector's spin-sensitivity. b) A  $70 \times 70 \mu\text{m}$  reflectivity image [white square in (a)], showing device features. c) A Kerr-rotation image of the optically-injected spin polarization ( $B_x=0$ ). d) Raw spin-detection data at 10 K,  $\Delta V_d(B_x)$ , at various  $V_d$ . e) The spin-detection sensitivity versus  $V_d$ .

with respect to the Fe magnetization  $\mathbf{M}$  ( $\parallel \pm \hat{y}$ ) by small applied fields  $\pm B_x$ . Using scanning Kerr-rotation microscopy [20, 21, 22], Figs. 1(b,c) show images of the reflectivity, and of the optically-injected spin polarization diffusing to the right and also to the left towards the spin detector. This additional polarization modifies the chemical potentials  $\mu_{\uparrow,\downarrow}$  in the GaAs under the detector, which (at constant  $j$ ) modifies  $P_j$  and therefore changes  $V_d$  by an amount  $\Delta V_d$  that is a measure of the detector's spin-sensitivity. To explicitly measure spin-dependent changes, the laser is modulated from right-to left-circular polarization at 50 kHz, and  $\Delta V_d$  at this frequency is measured between the detector and a distant reference contact. Importantly, this approach avoids magnetic dichroism or hot electron artifacts because the spins are injected into the channel (rather than through the Fe contact), where they cool before diffusing. Using low laser power (5-20  $\mu\text{W}$ ), perturbations to  $\mu_{\uparrow} - \mu_{\downarrow}$  are kept small, of order 1  $\mu\text{V}$ .

Fig. 1(d) shows  $\Delta V_d$  versus  $B_x$  at different biases  $V_d$  across the Fe/GaAs detector. Effectively, we electrically detect the  $\hat{y}$  component of diffusing and precessing spins that are optically oriented initially along  $\pm \hat{z}$ . Thus, the

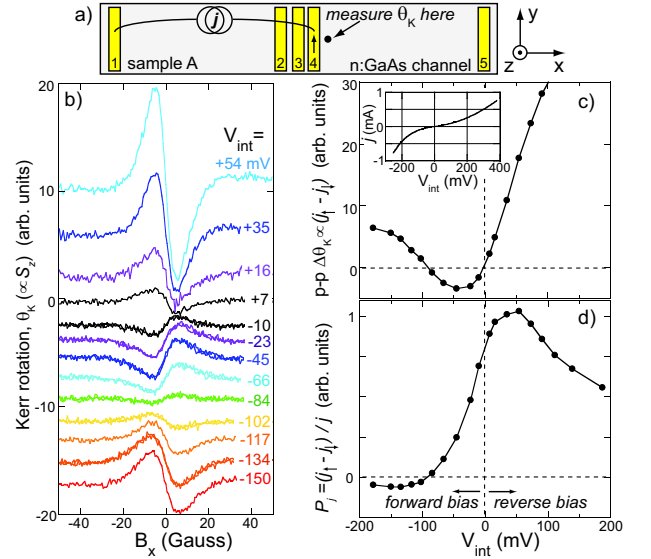


FIG. 2: a) Measuring  $P_j$ , the tunneling current polarization at contact 4 via spin injection at 10 K. Current  $j$  establishes a voltage bias  $V_{int}$  across the Fe/GaAs interface. b) Electrically-injected spins are measured via the Hanle-Kerr effect ( $\theta_K$  vs.  $B_x$ ), at different  $V_{int}$  (curves offset for clarity). c) The peak-to-peak Hanle amplitude,  $\Delta\theta_K \propto n_{\uparrow} - n_{\downarrow} \propto j_{\uparrow} - j_{\downarrow}$ , versus  $V_{int}$ . Inset:  $j(V_{int})$  for contact 4. d) Relative polarization of the tunneling current,  $P_j \propto (j_{\uparrow} - j_{\downarrow})/j$ , versus  $V_{int}$ .

curves exhibit antisymmetric “local Hanle” lineshapes which depend on spin lifetimes, diffusion constants, and source/detector separation [21, 22]. Maximum and minimum  $\Delta V_d$  occur at  $\pm B_x$  for which the injected spins have on average precessed  $\pm 90^\circ$  (parallel or antiparallel to  $\mathbf{M}$ ) before reaching the detector. Larger  $B_x$  causes rapid ensemble dephasing.

The peak-to-peak amplitudes of the  $\Delta V_d(B_x)$  curves [Fig. 1(e)] therefore provide a measurement of the electrical spin-detection sensitivity that depends only on the spin-dependent voltages induced by the remotely-injected spins. In sample A,  $\Delta V_d$  is clearly tunable with detector bias. It is large and positive near  $V_d=0$ , where additional minority polarization in the channel induces a positive  $\Delta V_d$  ( $\simeq +1.5 \mu\text{V}$ ) at the detection electrode. With increasing forward or reverse detector bias, however,  $\Delta V_d$  decreases and *inverts sign* – now, additional minority spins induce a *negative* voltage change. Electrons in GaAs with fixed spin can therefore be made to generate positive *or* negative voltage changes at epitaxial Fe/GaAs spin detectors, simply by tuning  $V_d$  by a few tens of mV. This freedom offers new routes (besides manipulating electron spins or contact magnetizations) to tune and switch spin-dependent electrical signals in semiconductor devices.

To understand the tunable spin detection sensitivity in sample A, it is essential to independently measure  $P_j$ , the polarization of the tunneling current that flows across

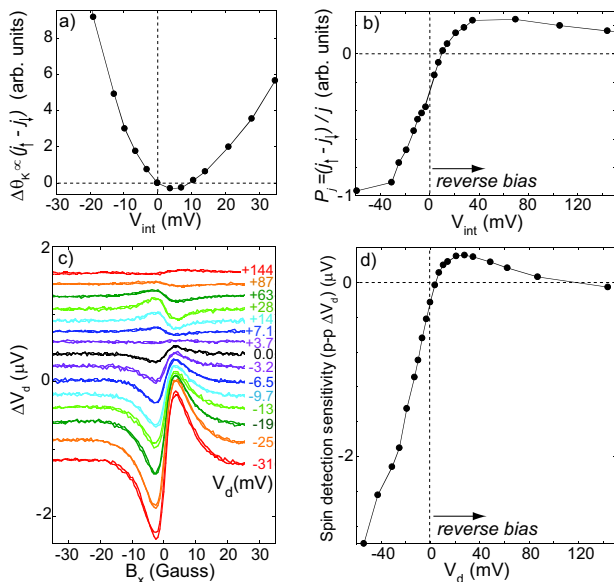


FIG. 3: Spin injection/detection data from sample B at 10 K. a) The electrically-injected spin polarization, measured by the Kerr effect  $\Delta\theta_K$  vs.  $V_{int}$ . b) Polarization of the tunneling current  $P_j$ , which now inverts under *reverse bias*, in contrast to sample A. c) Raw spin detection data,  $\Delta V_d(B_x)$  at various detector interface biases  $V_d$  (curves offset). d) The spin-detection sensitivity  $\Delta V_d$  versus  $V_d$ .

these biased Fe/GaAs interfaces. For this we measure the efficiency of electrical spin-*injection* using Kerr-rotation methods [20, 21, 22] (see Fig. 2). Here, a probe laser detects electrically-injected spins via the Hanle-Kerr effect,  $\theta_K$  ( $\propto S_z$ ) versus  $B_x$ , at a point in the channel  $\sim 10$   $\mu\text{m}$  to the right of an injecting contact (#4 again). For spins injected initially along  $\mathbf{M}$  ( $\pm\hat{y}$ ),  $\theta_K(B_x)$  curves exhibit similar lineshapes as seen in Fig. 1(d). Extrema occur at  $\pm B_x$  for which the spins have on average precessed  $\pm 90^\circ$  (to  $\pm\hat{z}$ ) at the detection point. A series of curves are shown in Fig. 2(b) at various injector interface biases,  $V_{int}$ . The curves invert at  $V_{int}=0$  and -90 mV. Their peak-to-peak amplitude  $\Delta\theta_K$  is proportional to majority- and minority-spin imbalance in the channel ( $n_\uparrow - n_\downarrow$ ), which in turn scales directly with the difference between majority- and minority-spin tunneling currents:  $\Delta\theta_K \propto j_\uparrow - j_\downarrow$ . Fig. 2(c) shows  $\Delta\theta_K(V_{int})$  and the current-voltage trace for contact 4. These optical data concur with all-electrical spin injection studies of these devices [5]. Normalizing by the total current  $j$  reveals the (relative) polarization of the tunneling current,  $P_j \propto (j_\uparrow - j_\downarrow)/j$  [see Fig. 2(d)].  $P_j$  clearly varies with  $V_{int}$ , showing a maximum near +50 mV and a sign inversion at -90 mV. All contacts on sample A and on other devices from this wafer show the same  $P_j$ .

Comparing sample A's spin-detection sensitivity  $\Delta V_d$  with  $P_j$  [Figs. 1(e) and 2(d)], general trends can be identified: Both exhibit a positive maximum near zero bias, and the inversion of  $\Delta V_d$  under small forward bias can

now be clearly explained by the inversion of  $P_j$  at similar bias. However, striking differences exist at large interface bias: Compared to  $P_j$ ,  $|\Delta V_d|$  is markedly enhanced under large forward bias, but is suppressed under large reverse bias.  $\Delta V_d$  also inverts sign *again* when  $V_{int} > +130$  mV, which is unexpected and cannot be inferred from  $P_j$ . Thus, spin-detection sensitivities in these Fe/GaAs structures do not simply track  $P_j$ , and their strong deviation at large biases suggests the nontrivial role of electric fields in the semiconductor channel (discussed below).

Data from heterostructure B are shown in Fig. 3. Unlike sample A, injection studies [Figs. 3(a,b)] show that  $P_j$  is dominated by *minority* spins near zero bias, and that  $P_j$  inverts at finite *reverse bias* ( $\sim +10$  mV). These differences likely originate in the microscopic details of their Fe/GaAs interfaces. Nonetheless,  $\Delta V_d$  of sample B [Figs. 3(c,d)] can be correlated with  $P_j$ . At zero bias, minority spins now generate small *negative* voltage changes at detection contacts ( $\Delta V_d \simeq -0.2$   $\mu\text{V}$ ), and  $\Delta V_d$  inverts sign at small reverse detector bias ( $V_d \simeq +5$  mV), as predicted from the similar inversion of  $P_j$ . However, like sample A,  $\Delta V_d$  markedly diverges from  $P_j$  at large bias, showing a suppression (and unexpected sign inversion) under large reverse detector bias, and a large enhancement under forward bias. Under forward bias  $|\Delta V_d|$  increases over tenfold, transforming sample B from a poor zero-bias spin detector into a much more sensitive spin detection device.

We can largely explain the striking differences between  $P_j$  and  $\Delta V_d$  at large bias within a 1-D model of spin transport effects and their influence on spin detection. As Fig. 4(a) depicts, a unit polarization  $p$  injected into the channel changes the spin densities  $n_{\uparrow,\downarrow}$  and potentials  $\mu_{\uparrow,\downarrow}$  at a nearby Fe/GaAs detector. At a fixed net interface current  $j$ , these changes modify  $P_j$ . Because  $G_{\uparrow,\downarrow}$  are in general unequal, we can derive the detector voltage change:  $\Delta V_d \propto k \frac{j \partial P_j}{\partial p} = k \left[ eD \frac{\partial}{\partial p} \left[ \frac{\partial(n_\uparrow - n_\downarrow)}{\partial x} \right] + e\mu E \frac{\partial}{\partial p} (n_\uparrow - n_\downarrow) \right]$ , where  $k = \frac{1}{4} \left( \frac{1}{G_\uparrow} - \frac{1}{G_\downarrow} \right)$ ,  $D$  is the electron diffusion constant,  $E$  is the channel electric field, and  $n_\uparrow - n_\downarrow$  and its gradient are evaluated at the interface. Using the spin transport model of [13] and the full spin-drift-diffusion equations [23], we find that  $\Delta V_d$  can deviate markedly from  $P_j$  due to two effects: i) drift and diffusion terms oppose each other in reverse bias but add in forward bias; and ii)  $E$  drifts  $p$  away from (towards) the detector in reverse (forward) bias. These transport effects are normally superimposed on the bias dependence of  $P_j$  itself, but are disentangled in Fig. 4(b) by showing  $\Delta V_d$  calculated for a constant  $P_j$ . Drift can enhance or suppress  $\Delta V_d$  relative to  $P_j$  under forward or reverse detector bias, by an amount that depends sensitively on the channel conductivity. In the metallic limit,  $\Delta V_d(V_d)$  tracks  $P_j$  exactly, because  $E \sim 0$ . Notably, this model suggests that spin-detection sensitivities can also be controlled (inde-

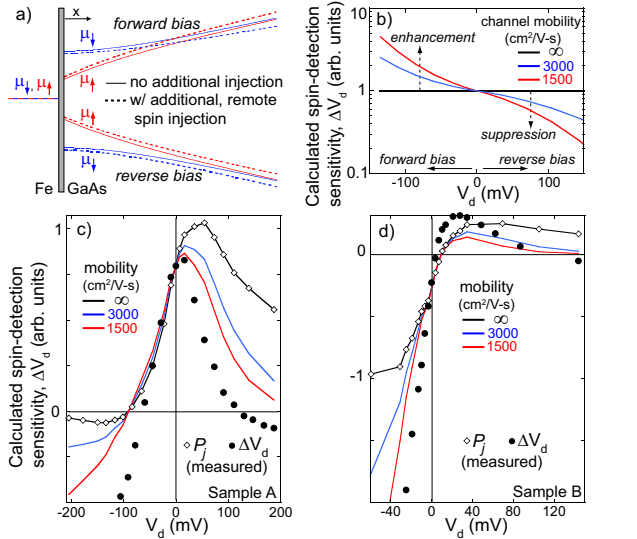


FIG. 4: a) Schematic of  $\mu_{\uparrow,\downarrow}$  near a Fe/GaAs spin detector under forward/reverse bias  $V_d$  (solid lines). Dotted lines show  $\mu_{\uparrow,\downarrow}$  modified by a remotely-injected spin polarization. b) Calculated  $\Delta V_d$  of a detector with bias-independent  $P_j$ . Enhancement and suppression are due to spin drift in the channel. c,d) Calculated  $\Delta V_d$  for sample A and B, using measured  $P_j$  (open symbols) as inputs, and a polarization source 20  $\mu\text{m}$  away.  $\Delta V_d$  is calculated for three channel conductivities, by varying the electron mobility  $\mu$ .

pendent of  $P_j$ ) by engineering channel conductivities.

Figures 4(c,d) show  $\Delta V_d$  calculated for sample A and B using  $G_{\uparrow,\downarrow}$  determined from  $P_j$  and  $j(V_{int})$  data. Electron densities and spin lifetimes are measured independently. The results (in arbitrary units) are scaled so that  $\Delta V_d \equiv P_j$  at zero bias. For realistic  $n$ :GaAs channel mobilities the calculated  $|\Delta V_d|$  drops (increases) much more rapidly than  $P_j$  under large reverse (forward) bias, in good agreement with experimental  $\Delta V_d$  values (black points). However, the sign inversion of  $\Delta V_d$  observed at large reverse bias is not expected within this 1-D model, because drift and diffusion terms cancel exactly to leading order [24] suppressing  $\Delta V_d$  monotonically to zero. No such restriction exists, though, in more realistic 2-D or 3-D geometries, which allow for inhomogeneous  $E$  fields.

Within an overall scaling factor, measured  $\Delta V_d(V_d)$  curves [Figs. 3(d), 1(e)] are independent of the injection laser's power and location, suggesting that a spin detector's sensitivity can be freely tuned, independent of the spin injection source. This is demonstrated in Fig. 5

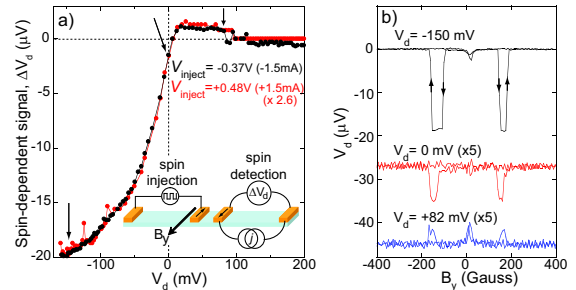


FIG. 5: a) Schematic shows all-electrical lateral spin-valve setup. Black (red) points show the spin-dependent change in detector voltage  $\Delta V_d$  versus detector bias  $V_d$  for a forward (reverse) biased spin injector. b) Raw spin-valve data at three detector biases [arrows in (a)], using a fixed -1.5 mA injector bias (offset for clarity). Note switching and ten-fold enhancement of the detected signal.

for the important case of all-electrical spin injection and detection. Here, non-local lateral spin-valve studies [5] were performed on a device with  $P_j$  similar to sample B. Fig. 5(a) shows the spin-valve signal versus detector bias, when the source electrode is forward- and reverse-biased (black and red points). The dependence on  $V_d$  is the same, confirming that a detector's sensitivity can be optimized independently of an injector's biasing. Fig. 5(b) shows raw spin-valve data with  $V_d = -150, 0,$  and  $+82$  mV, explicitly showing that detection sensitivities are tunable in both sign and magnitude in all-electrical devices.

In these studies, interfacial biases and channel electric fields both play essential roles. Because semiconductors can support large electric fields, it is possible to bias each device element – source, channel, and detector – independently. Controlling spin transport through both interfacial and bulk band structures represents a unique capability of ferromagnet-semiconductor devices that is only beginning to be explored. The authors acknowledge support from the Los Alamos LDRD program, ONR, NSF MRSEC, NNIN and IGERT programs, and JSTC (T.K.).

- 
- [1] I. Žutić, J. Fabian, and S. Das Sarma, *Rev. Mod. Phys.* **76**, 323 (2004).
- [2] R. Jansen and B. C. Min, *Phys. Rev. Lett.* **99**, 246604 (2007).
- [3] P. R. Hammar and M. Johnson, *Phys. Rev. Lett.* **88**, 066806 (2002).
- [4] D. Saha, M. Holub, and P. Bhattacharya, *Appl. Phys. Lett.* **91**, 072513 (2007).
- [5] X. Lou *et al.*, *Nat. Phys.* **3**, 197 (2007).
- [6] I. Appelbaum, B. Huang, and D. J. Monsma, *Nature* **447**, 295 (2007).
- [7] O. M. J. van 't Erve *et al.*, *Appl. Phys. Lett.* **91**, 212109 (2007).
- [8] N. Tombros *et al.*, *Nature* **448**, 571 (2007).
- [9] A. Fert and H. Jaffrès, *Phys. Rev. B* **64**, 184420 (2001).
- [10] F. J. Jedema *et al.*, *Nature* **416**, 713 (2002).
- [11] S. O. Valenzuela *et al.*, *Phys. Rev. Lett.* **94**, 196601 (2005).
- [12] E. I. Rashba, *Phys. Rev. B* **62**, R16267 (2000).
- [13] D. L. Smith and R. N. Silver, *Phys. Rev. B* **64**, 045323 (2001).
- [14] J. Moser *et al.*, *Appl. Phys. Lett.* **89**, 162106 (2006).
- [15] H. Dery and L. J. Sham, *Phys. Rev. Lett.* **98**, 046602 (2007).
- [16] A. N. Chantis *et al.*, *Phys. Rev. Lett.* **99**, 196603 (2007).
- [17] Z. G. Yu and M. E. Flatté, *Phys. Rev. B* **66**, 201202(R) (2002).
- [18] G. Schmidt *et al.*, *Phys. Rev. Lett.* **92**, 226602 (2004).
- [19] A. T. Hanbicki *et al.*, *Appl. Phys. Lett.* **82**, 4092 (2003).
- [20] J. Stephens *et al.*, *Phys. Rev. Lett.* **93**, 097602 (2004).
- [21] S. A. Crooker *et al.*, *Science* **309**, 2191 (2005).
- [22] M. Furis *et al.*, *New J. Phys.* **9**, 347 (2007).
- [23] M. Hruška *et al.*, *Phys. Rev. B* **73**, 075306 (2006).
- [24] A. N. Chantis and D. L. Smith, To be published.